In Vivo Packaging of Triacylglycerols Enhances Arabidopsis Leaf Biomass and Energy Density[1][W][OA]

Somrutai Winichayakul, Richard William Scott, Marissa Roldan, Jean-Hugues Bertrand Hatier, Sam Livingston, Ruth Cookson, Amy Christina Curran, and Nicholas John Roberts*

AgResearch, Ltd., Grasslands Research Centre, Private Bag 11008, Palmerston North 4442, New Zealand (S.W., R.W.S., M.R., J.-H.B.H., S.L., R.C., A.C.C., N.J.R.); and Algenetix, Inc., San Diego, California 92121 (A.C.C., N.J.R.)

Our dependency on reduced carbon for energy has led to a rapid increase in the search for sustainable alternatives and a call to focus on energy densification and increasing biomass yields. In this study, we generated a uniquely stabilized plant structural protein (cysteine [Cys]-oleosin) that encapsulates triacylglycerol (TAG). When coexpressed with diacylglycerol *O*-acyltransferase (DGAT1) in Arabidopsis (*Arabidopsis thaliana*), we observed a 24% increase in the carbon dioxide (CO_2) assimilation rate per unit of leaf area and a 50% increase in leaf biomass as well as approximately 2-, 3-, and 5-fold increases in the fatty acid content of the mature leaves, senescing leaves, and roots, respectively. We propose that the coexpression led to the formation of enduring lipid droplets that prevented the futile cycle of TAG biosynthesis/lipolysis and instead created a sustained demand for de novo lipid biosynthesis, which in turn elevated CO_2 recycling in the chloroplast. Fatty acid profile analysis indicated that the formation of TAG involved acyl cycling in Arabidopsis leaves and roots. We also demonstrate that the combination of Cys-oleosin and DGAT1 resulted in the highest accumulation of fatty acids in the model single-cell eukaryote, *Saccharomyces cerevisiae*. Our results support the notion that the prevention of lipolysis is vital to enabling TAG accumulation in vegetative tissues and confirm the earlier speculation that elevating fatty acid biosynthesis in the leaf would lead to an increase in CO_2 assimilation. The Cys-oleosins have applications in biofuels, animal feed, and human nutrition as well as in providing a tool for investigating fatty acid biosynthesis and catabolism.

Although liquid biofuels offer considerable promise, the reality of utilizing biological material is tempered by competing uses and the quantities available. Triacylglycerol (TAG) is a neutral lipid with twice the energy density of cellulose and can be used to generate biodiesel, a high-energy-density desirable biofuel with one of the simplest and most efficient manufacturing processes (Hill et al., 2006; Granda et al., 2007; Somerville, 2007; Fortman et al., 2008; Ohlrogge et al., 2009; Chapman et al., 2013; Troncoso-Ponce et al., 2013). Consequently, engineering plants to accumulate TAG in vegetative tissues and elevating the TAG content of oleaginous yeast and bacteria is the focus of multiple research groups (Fortman et al., 2008; Ohlrogge et al., 2009; Chapman et al., 2013; Troncoso-Ponce et al., 2013).

A variety of strategies to engineer TAG accumulation in vegetative tissues and microorganisms have been explored. These include the stimulation of fatty acid biosynthesis and TAG production by overexpressing seed development transcription factors *LEAFY COTYLEDON1* (*LEC1*), *LEC2*, and *WRINKLED1* (*WRI1*) in planta (Mu et al., 2008; Santos-Mendoza et al., 2008; Andrianov et al., 2010; Sanjaya et al., 2011) and the direct up-regulation of the Kennedy pathway (Kennedy, 1961) in both plants and yeast (Bouvier-Navé et al., 2000; Durrett et al., 2008; Andrianov et al., 2010; Beopoulos et al., 2011) by overexpressing the enzyme responsible for the last and only committed step in TAG biosynthesis, diacylglycerol *O*-acyltransferase (DGAT [EC 2.3.1.20]. Furthermore, substantial gains have been made by other approaches, including the silencing of the Arabidopsis gene *APS1* (At5g48300; a key gene involved in starch biosynthesis; Sanjaya et al., 2011), mutation of *CGI-58* (a regulator of neutral lipid accumulation; James et al., 2010), and overexpression of mammalian monoacyglycerol acyltransferase in tobacco (*Nicotiana tabacum*) leaves (Petrie et al., 2012).

Leaf TAG is used as a short-term storage intermediate of thylakoid lipid during ongoing membrane turnover, remodeling, and senescence (Kaup et al., 2002; Athenstaedt and Daum, 2006; Lin and Oliver, 2008; Slocombe et al., 2009; James et al., 2010; Chapman et al., 2013; Troncoso-Ponce et al., 2013). For example, Arabidopsis (*Arabidopsis thaliana*) leaves lose 1.6% of fatty acids per day during senescence, yet the TAG levels are less than 1% of total lipids at all stages (Yang and Ohlrogge, 2009). Hence, despite the impressive gains in manipulating TAG levels in vegetative tissues (5-

[1] This work was supported by the New Zealand Ministry of Business, Innovation, and Employment (contract nos. C10X0203 and C10X0815), AgResearch PreSeed (contract no. 18), AGMARDT (grant no. 990), and Algenetix (contract no. A15596).

* Corresponding author; e-mail nick.roberts@agresearch.co.nz.

The author responsible for distribution of materials integral to the findings presented in this article in accordance with the policy described in the Instructions for Authors (www.plantphysiol.org) is: Nicholas John Roberts (nick.roberts@agresearch.co.nz).

[W] The online version of this article contains Web-only data.

[OA] Open Access articles can be viewed online without a subscription.

www.plantphysiol.org/cgi/doi/10.1104/pp.113.216820

to 20-fold in leaves) and microorganisms, it has been acknowledged that to achieve further increases in TAG, preventing its catabolism may be crucial within nonoleaginous tissues and over a range of developmental stages (Ohlrogge et al., 2009; Slocombe et al., 2009; Yang and Ohlrogge, 2009; James et al., 2010; Troncoso-Ponce et al., 2013). Given the conserved nature of eukaryotic neutral lipid metabolism, the yeasts are recognized as an excellent model for studying synthesis, storage, and turnover (Czabany et al., 2007). Moreover, their rate of biomass production combined with the fact that they do not displace traditional crops makes them an attractive alternative for the potential production of TAGs. However, in contrast to leaves, yeasts accumulate neutral lipids (both TAG and sterol esters) as starting materials for membrane lipid synthesis rather than as an energy reserve (Czabany et al., 2007). Furthermore, neutral lipid accumulation in unicellulates typically only occurs in the stationary phase, and as such, producing and accumulating TAG earlier in the growth curve is a high priority (Chisti, 2007; Granda et al., 2007; Fortman et al., 2008; Beopoulos et al., 2011).

Substantial quantities of neutral lipids (TAGs, sterol esters, and wax esters) are unable to integrate into lipid bilayers; instead, they form the hydrophobic core of ubiquitous, dynamic organelles called lipid droplets (LDs; Athenstaedt and Daum, 2006). In eukaryotes, these relatively simple but specialized storage organelles are generally thought to originate from the endoplasmic reticulum (ER), where the neutral lipids accumulate between the two leaflets of the ER membrane. Eventually, they form droplets that are released via a budding mechanism into the cytoplasm (Athenstaedt and Daum, 2006; Martin and Parton, 2006). The hydrophobic core of the LD is surrounded by a phospholipid monolayer with a small number of embedded proteins (Welte, 2007), including sterol ester hydrolases in yeast (Athenstaedt and Daum, 2006) and TAG lipases in both plants (Eastmond, 2006) and yeast (Athenstaedt and Daum, 2006). The breakdown of TAG in both plants and yeast is achieved by lipases, which results in the release of free fatty acid and diacylglycerol (DAG). The biological roles and redundancy of the lipases, however, suggest that in any one organism, exercising control over these in specific tissues is likely to be a difficult task (Athenstaedt and Daum, 2006; Czabany et al., 2007; Yang and Ohlrogge, 2009; Troncoso-Ponce et al., 2013).

In contrast to leaves and yeast, seeds store TAG as a long-term energy supply; this is achieved with the aid of a distinctive proteinaceous emulsifier called oleosin that coats the outside of the LDs (commonly referred to as oil bodies; Tzen et al., 1992). Two isoforms of oleosin (H and L) were reported to be present in diverse angiosperms; the H-oleosins possess an insertion of 18 residues downstream of the conserved central hydrophobic domain (Tai et al., 2002). Oleosins prevent the accidental exposure to lipases and inhibit LD coalescence during desiccation, freezing, and germination (Tzen et al., 1992; Siloto et al., 2006; Shimada et al., 2008). They also appear to act as docking and/or activating proteins for TAG lipases (Athenstaedt and Daum, 2006). Although desiccation is not a factor in most animal cells, a similar role in LD protection and controlled lipolysis is attributed to the perilipins in animal adipocyte and steroidogenic cells and to the adipophilins in all other tissues (Athenstaedt and Daum, 2006; Martin and Parton, 2006; Brasaemle, 2007; Goodman, 2008; Murphy, 2012). Yeasts, however, contain no homologs of oleosins or perilipins, yet the oleaginous yeast species can accumulate more than 20% lipid as a fraction of the dry weight (Beopoulos et al., 2011).

We previously suggested that the coexpression of DGAT1 and oleosin in leaves may result in the formation of LDs and, subsequently, enable the long-term accumulation of TAG (Winichayakul et al., 2008); this suggestion has been recently reiterated by others (Dyer et al., 2012). In order to be effective, however, the recombinant oleosin would have to lead to the formation of LDs that are able to prevent lipase entry for the life of the leaf and preferably during senescence, where it has been reported that a large proportion of the ESTs expressed during senescence are from genes involved in proteolysis, in particular, Cys proteases (Gepstein, 2004).

The generally accepted topology of oleosin is one in which the N- and C-terminal amphipathic arms are arranged on the surface of the LD while the central hydrophobic domain protrudes through the phospholipid monolayer into the TAG core (Tzen et al., 1992). Earlier, we demonstrated that even when only a fraction (less than 2%) of seed LD protein consisted of engineered tandem head-to-tail repeats of oleosin (polyoleosin), the LD integrity was enhanced both in planta and in vitro (Scott et al., 2010). Seed germination was slightly delayed but could be overcome by the addition of Glc (Scott et al., 2010). In vitro exposure of these LDs to Ser protease showed that (compared with native LDs) the TAG was contained for a prolonged period and yet the amphipathic arms of the oleosins (including those of polyoleosin) were rapidly degraded (Scott et al., 2010). Combined, these results indicate that during seed germination, lipase entry was likely delayed but not prevented. Furthermore, while polyoleosin was detected in the seed, it was not found in the leaves, suggesting that expression in these organs could also be a limiting factor.

An alternative way to stabilize LDs may be to cross link the amphipathic arms of the oleosins; this has already been demonstrated in vitro by the chemical cross linking of artificial LDs with either gluteraldehyde or genipin (Peng et al., 2003). Recently, the sesame seed (*Sesamum indicum*) H-oleosin but not the L-oleosin was found to be ubiquitinated shortly after germination, and two of the three confirmed ubiquitination sites were located in the H-domain (Hsiao and Tzen, 2011). Consequently, we asked if we could produce cross-linked L-oleosins both in planta and in yeast to generate stable LDs. In this report, we describe the effect of coexpressing DGAT1 and L-oleosin engineered to contain different numbers of strategically placed Cys residues (Cys-oleosin). We show that one of the Cys-oleosins led to the long-term elevation of fatty acid content and the

accumulation of TAG in leaves and roots and elevated the fatty acid content of yeast. The Cys-oleosin was found to be targeted to and cross linked in leaf and root LDs, making them highly resistant to Cys protease. Infrared gas analysis revealed that the accumulation of the Cys-oleosin in the leaf not only correlated with increases in TAG but also in leaf biomass and CO_2 assimilation rate. We provide a potential mechanism to explain this phenomenon.

RESULTS

Oleosins Were Engineered to Contain up to 13 Cys Residues in the Amphipathic Arms

The conserved length and sequence of oleosin hydrophobic cores contrast with the diversity of their N- and C-terminal amphipathic regions. Perhaps with the exception of the predicted amphipathic α-helix immediately downstream of the hydrophobic domain (Tzen et al., 1992), the diversity suggests that their length and specific sequence are somewhat unimportant in the maintenance of integrity. Instead, it may be the balance and distribution of charge and hydrophobicity that allow the amphipathic regions to interact appropriately with both the aqueous environment and polar heads of the phospholipid monolayer. In the oleosin topology model of Tzen et al. (1992), it was proposed that the amphipathic arms lie on the surface of the LDs, with the positively and negatively charged amino acids distributed along the arms separated by neutral residues. The negatively charged residues are exposed to the exterior, while the positively charged residues face the interior (Tzen et al., 1992). The natural occurrence of Cys residues in the amphipathic arms of oleosins appears to be either nonexistent or extremely rare.

To generate Cys-oleosins, we engineered between one and seven Cys residues into each amphipathic arm of the 15-kD sesame L-oleosin (accession no. AAD42942; Fig. 1). These were labeled o0-0, o1-1, o3-1, o1-3, o3-3, o5-6, and o6-7; "o" stands for oleosin, and the first and second numerals denote the number of Cys residues in the N- and C-terminal amphipathic arms, respectively. The native oleosin (o0-0) serves as a control. The Cys residues were positioned to both maximize their potential to form interoleosin disulfide bonds and to minimize disruption of the envisaged association between the amphipathic arms and the LD surface (Tzen et al., 1992). In the o1-1, o3-1, o1-3, and o3-3 constructs, the Cys residues were relatively evenly spaced and substituted for existing predicted surface hydrophilic residues, leaving the majority of charged residues unchanged and eight to 12 native residues between each substitution (Fig. 1). To maintain a relatively even spacing between the Cys residues and not further disrupt the predicted charge balance of the amphipathic arms, the synthesis of o5-6 and o6-7 was achieved by the addition of Cys residues to the existing o3-3 backbone. Furthermore, the N-terminal Cys of the o6-7 construct was accomplished by repeating the six N-terminal residues of the o5-6 construct (Fig. 1). In the o5-6 and o6-7 constructs, an additional Gly was also included to provide flexibility between the introduced Cys residue and the N-terminal amphipathic arm quadruple Gln repeat. Consequently, the spacing between the Cys residues on the o5-6 and o6-7 hydrophilic arms was approximately half that of the o3-3, and their amphipathic arms were longer.

Vegetative Tissues Coexpressing DGAT1 and Cys-Oleosin Have a Higher Fatty Acid Content and Accumulate TAG

Total fatty acid levels for leaves harvested 14, 21, and 35 d after sowing (DAS) are shown for the highest accumulating lines from the wild type, vector control, DGAT1 alone (D1), and DGAT1 coexpressed with o0-0, o1-1, o3-1, o1-3, or o3-3 (D1o0-0, D1o1-1, D1o1-3, D1o3-1, and D1o3-3, respectively; Table I). At 14 DAS, there was no significant difference between the fatty acid levels of the wild-type, vector control, or D1 leaves. In contrast, plants coexpressing DGAT1 and oleosin (except D1o1-1) had significantly more (6%–34%) leaf fatty acid. The highest levels occurred in those plants transformed with oleosin containing four or more Cys residues (D1o1-3, D1o3-1, and D1o3-3), which also correlated with the accumulation of TAG (Supplemental Fig. S1). Except for the D1o3-3 plants, the leaf fatty acid levels declined dramatically between 14 and 21 DAS, and in most plants, there was a further small reduction between 21 and 35 DAS (Table I). The reduction also corresponded with reduced levels of

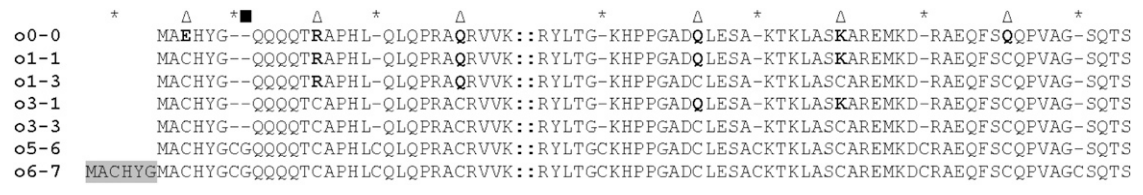

Figure 1. Positions of Cys residues engineered into different Cys-oleosins. Triangles indicate engineered Cys residues substituting for existing (boldface) residues; asterisks indicate Cys residues engineered in addition to the original peptide sequence; the square indicates a Gly residue added to both o5-6 and o6-7. Gray shading indicates the duplicated N-terminal residues added to o6-7, and double colons indicate the hydrophobic domain (72 residues in total). Gaps (dashes) have been added to keep sequences aligned.

Table I. *Total lipid content (% of dry weight) of homozygous transgenic and control leaves harvested 14, 21, and 35 DAS*

Values represent means ± SD from separate analyses ($n = 6$). Parentheses show P values for statistical significance between the transgenic line and the wild type calculated by Student's two-tailed t test. N/A, Not available; ns, not significant.

Construct	Plant Age		
	14 DAS	21 DAS	35 DAS
Wild type	5.0 ± 0.3	3.8 ± 0.05	3.7 ± 0.2
Vector control	4.8 ± 0.2 (ns)	4.0 ± 0.1 ($P = 0.0429$)	3.9 ± 0.1 ($P = 0.0231$)
D1	4.8 ± 0.2 (ns)	3.8 ± 0.02 (ns)	3.7 ± 0.01 (ns)
D1o0-0	5.3 ± 0.1 ($P = 0.0319$)	3.8 ± 0.05 (ns)	4.0 ± 0.03 ($P = 0.0019$)
D1o1-1	5.1 ± 0.1 (ns)	4.1 ± 0.1 ($P = 0.0004$)	3.7 ± 0.2 (ns)
D1o1-3	5.5 ± 0.1 ($P = 0.0013$)	4.3 ± 0.3 ($P = 0.0016$)	4.1 ± 0.03 ($P = 0.0002$)
D1o3-1	5.9 ± 0.2 ($P = 0.0001$)	4.3 ± 0.2 ($P = 2.7E-05$)	4.3 ± 0.2 ($P = 0.0003$)
D1o3-3	6.7 ± 0.1 ($P = 5.3E-08$)	6.8 ± 0.1 ($P = 5.6E-13$)	7.0 ± 0.2 ($P = 1.5E-11$)
D1o5-6	N/A	N/A	4.5 ± 0.02 ($P = 3.4E-07$)
D1o6-7	N/A	N/A	4.5 ± 0.08 ($P = 1.1E-06$)

TAG in the D1o1-3 and D1o3-1 plants. On the other hand, the fatty acid content of the D1o3-3 leaves continued to rise until 35 DAS (approximately 190% greater than in the wild type). The gross energy of D1o3-3 and wild-type leaves 14 DAS was determined to be 16.4 and 15.6 kJ g^{-1}, respectively, and by 35 DAS, this declined to 14.7 and 14.0 kJ g^{-1}, respectively. From 49 to 91 DAS (fully senescent), the fatty acid content of D1o3-3 leaves dropped steadily, but not to the same degree as in the wild type. At full senescence, the fatty acid content was 340% greater than in equivalent aged wild-type leaves (Fig. 2, A and B). Furthermore, direct analysis of TAG by gas chromatography-mass spectrometry indicated that in the D1o3-3 leaves, the TAG level did not begin to decrease until 63 DAS and was still present in the senescent leaf (Fig. 2C). TAG accumulation was also seen by confocal microscopy, where numerous droplets of neutral lipids were seen in the cells of D1o3-3 leaves but not in the wild type (Fig. 2D).

In the case of the plants coexpressing DGAT1 and o5-6 or o6-7 (D1o5-6 or D1o6-7, respectively), the highest leaf fatty acid occurred in hemizygous plants that failed to produce viable homozygous seed. The majority of D1o5-6 and D1o6-7 cotyledons and subsequent true leaves developed interveinal chlorosis 14 d after germination on one-half-strength Murashige and Skoog medium + 1% Suc (Supplemental Fig. S2). This could be prevented to some degree by germinating on medium containing higher levels of Murashige and Skoog medium (1× and 1.5×), although many seedlings did not develop past the second-leaf stage. Of those that did survive, we were able to generate homozygous lines and analyze for fatty acid content (Table I); however, the leaves of these lines had a distinctly raised punctuated adaxial surface, elongated petioles, and downward-rolling leaf margins (Supplemental Fig. S2). Consequently, we chose not to pursue further analysis of the D1o5-6 and D1o6-7 lines.

Since the expression of both DGAT1 and o3-3 was driven by constitutive promoters, we also compared the total fatty acid content of the roots 35 DAS and found this to be 8.2% ± 0.2% and 1.7% ± 0.2% dry weight in the D1o3-3 and wild-type samples, respectively. Hydrophobic column chromatography-quantitative fatty acid methyl esters revealed that all of the additional fatty acid in the roots was in the form of TAG (6.5% ± 0.2% dry weight), whereas in the leaf, TAG constituted approximately 65% of the additional fatty acid (2.1% ± 0.1% dry weight). Integration from the direct analysis of TAG by gas chromatography-mass spectrometry showed that on a dry weight basis, the roots contained three times more TAG than leaves (Supplemental Fig. S3). This technique also suggested that some of the additional fatty acids in the leaf appeared to be in the form of more polar glycerolipids (Supplemental Fig. S4).

Accumulation of TAG Changes the Fatty Acid Profile

Compared with the wild type, the overexpression of DGAT1 alone did not have a significant impact on the fatty acid profile of the leaves 35 DAS, and while the D1o0-0 leaves had a marginal but significant decrease in the proportion of 16:1, this was also seen in the vector control (Table II). The coexpression of DGAT1 and any of the Cys-oleosins, however, resulted in highly significant changes to the profile. This included increases in the proportions of leaf 18:1 and 18:2 and decreases in 16:0, 16:1, 16:3, and 18:3; in each case, the greatest changes occurred in the D1o3-3 plants (Table II). Furthermore, the very-long-chain fatty acids (VLCFAs) 20:1, 22:0, 24:0, and 24:1 were detected in D1o3-3 leaves but not in any other plants. The differences between the wild-type and D1o3-3 leaf fatty acid profiles reflected the profile of the purified TAG from the D1o3-3 leaves (Table II).

Like the D1o3-3 leaves, the fatty acid profile of the D1o3-3 roots showed highly significant increases in the proportions of 18:1 and 18:2 and decreases in 16:0 and 18:3 (Table II). In contrast with the leaves, however, the proportion of 16:1 was not significantly different, and 16:3 was not detected. 18:0 was only detected in

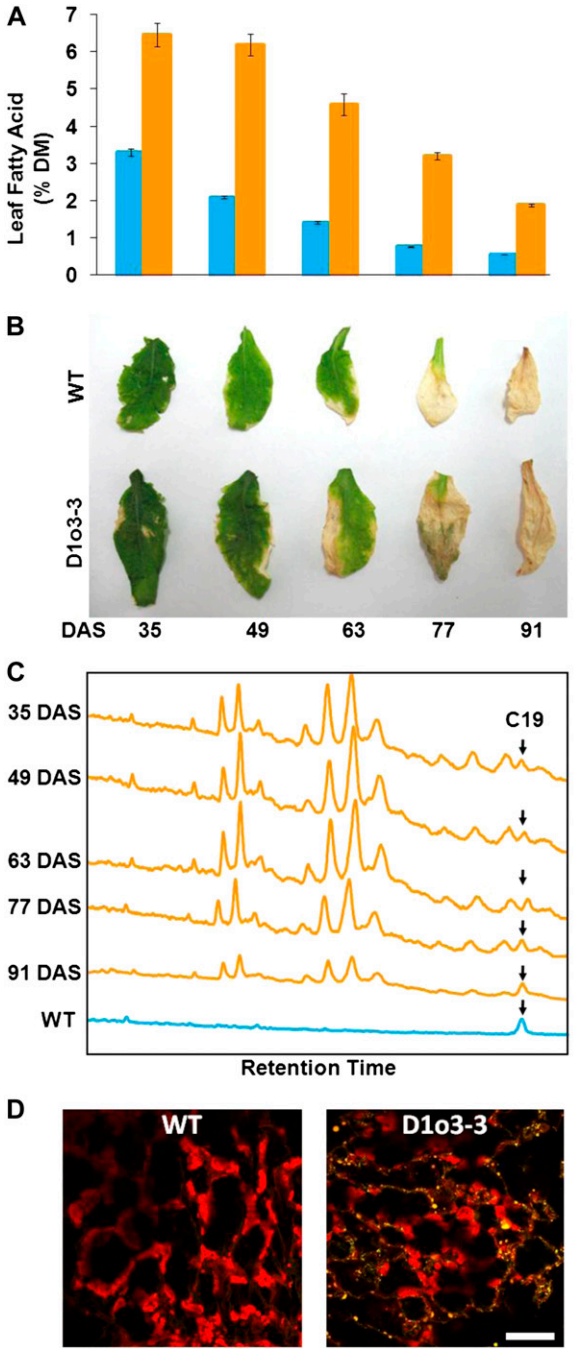

Figure 2. Accumulation of total fatty acids and TAG in D1o3-3 leaves over time. A, Total fatty acid content (as a percentage of dry matter [DM]) of wild-type (blue bars) and D1o3-3 (orange bars) leaves from 35, 49, 63, 77, and 91 DAS. Bars represent mean values ± SD of separate experiments ($n = 5$), with statistical significance between the wild type and D1o3-3 calculated by Student's two-tailed t test. At 35, 49, 63, 77, and 91 DAS, $P = 7.65$ E-09, 3.58 E-10, 3.22 E-09, 4.44 E-12, and 1.14 E-12, respectively. B, Typical leaf appearance from the wild type (WT) and D1o3-3 at 35 to 91 DAS. C, Overlaid total ion chromatogram traces of TAGs extracted from equal quantities of freeze-dried leaf material from the wild type at 35 DAS (blue trace) or D1o3-3 at 35 to 91 DAS (orange traces). Arrows indicates the C19 TAG internal standard. D, Confocal image of Nile Red-stained wild-type and D1o3-3 leaves (approximately 21 DAS); neutral lipids are seen as yellow fluorescence. Bar = 50 μm.

roots, and the proportion of this was increased highly significantly in the D1o3-3 plants. The VLCFAs 22:0 and 24:0 were present in the roots of both the wild type and D1o3-3; however, 20:1 and 24:1 were only detected in the D1o3-3 roots. As per the leaves, the differences between the fatty acid profiles of wild-type and D1o3-3 roots reflected the profile of the purified TAG from the D1o3-3 roots (Table II).

D1o3-3 Plants Have Elevated CO_2 Assimilation and Leaf Biomass

The transgenic lines were visually indistinguishable from the wild type, except for the D1o3-3 plants, which grew more vigorously and had larger leaves (Fig. 2B) as well as a modest delay (2–3 d) in inflorescence emergence (Fig. 3E). However, over multiple comparative plantings, there were no obvious differences in seed germination, seedling growth, the completion of flower production and development, seed maturation, or the onset and rate of leaf senescence (Fig. 2B). Infrared gas analysis measurements on plants during the middle of their flower production (35 DAS) showed that the D1o3-3 plants were assimilating up to 24% more CO_2 m^{-2} s^{-1} than wild-type plants (Fig. 3D). The elevated CO_2 assimilation rate led to an approximately 50% increase in leaf biomass at 25 DAS (floral stalk emergence in the wild type), where the average leaf biomass of the highest fatty acid-accumulating D1o3-3 line (D1o3-3#47) and the wild type was 47.6 ± 4.4 and 30.9 ± 3.5 mg dry weight per plant, respectively. From 25 to 35 DAS, the plants continued to grow, and the leaf biomass of the D1o3-3 plants remained approximately 50% greater than in the wild type (90.0 ± 6.1 and 61.1 ± 3.3 mg dry weight per plant, respectively; $n = 50$). Comparisons between independent D1o3-3 lines indicate that there was a positive correlation between the accumulation of recombinant o3-3 Cys-oleosin, leaf fatty acid content, TAG accumulation, and CO_2 assimilation rate (Fig. 3). By comparison, overexpression of DGAT1 and unmodified oleosin (D1o0-0) resulted in only a modest elevation of leaf lipid but did not have any impact on the leaf CO_2 assimilation (Fig. 3).

DGAT1 + Cys-Oleosin Elevated the Accumulation of TAG in Yeast Cells

To assess the influence of Cys-oleosin on fatty acid accumulation in the model yeast *Saccharomyces cerevisiae*, we compared three constitutive expression constructs in the strain INV Sc 1 (Life Technologies). These were Arabidopsis DGAT1 (AtD), AtD plus native oleosin (AtD+o0-0), and AtD plus oleosin with three Cys residues per amphipathic arm (AtD+o3-3); all open reading frames were optimized for expression in yeast. Cultures expressing these constructs had similar growth curves (Fig. 4A); however, the highest fatty acid contents and production rates were always in the following order: AtD+o3-3 > AtD+o0-0 > AtD. By the late stationary

Table II. *Fatty acid profiles of leaf total fatty acid (L), leaf TAG (L-TAG), root total fatty acid (R), and root TAG (R-TAG) from material harvested 35 DAS*

Values represent mean percentages of total fatty acids ± SD from separate analysis ($n = 6$ for total fatty acid profiling in both leaves and roots, $n = 4$ for TAG profiling in both leaves and roots). Parentheses show P values for statistical significance between the transgenic line and the wild type calculated by Student's two-tailed t test. nd, Not detected; ns, not significant.

Construct	C16:0	C16:1	C16:3	C18:0	C18:1	C18:2	C18:3	C20:1	C22:0	C24:0	C24:1
Wild type (L)	17.2 ± 0.9	4 ± 0.2	11.3 ± 0.9	nd	1.6 ± 0.1	11.8 ± 1.1	54.2 ± 4.2	nd	nd	nd	nd
Vector control (L)	16.6 ± 0.4 (ns)	3.6 ± 0.1 ($P = 0.0126$)	11.5 ± 0.5 (ns)	nd	1.5 ± 0.1 (ns)	12.2 ± 0.3 (ns)	54.6 ± 1.3 (ns)	nd	nd	nd	nd
D1 (L)	16.4 ± 1.6 (ns)	3.5 ± 0.6 (ns)	11.5 ± 1.6 (ns)	nd	1.6 ± 0.4 (ns)	12.6 ± 1.9 (ns)	54.4 ± 7 (ns)	nd	nd	nd	nd
D1o0-0 (L)	17 ± 1.3 (ns)	3.5 ± 0.4 ($P = 0.0173$)	11.8 ± 1.2 (ns)	nd	1.5 ± 0.3 (ns)	11.2 ± 0.8 (ns)	54.6 ± 5.5 (ns)	nd	nd	nd	nd
D1o1-1 (L)	16.8 ± 0.7 (ns)	3.5 ± 0.4 (ns)	13.3 ± 1 ($P = 0.0106$)	nd	4.6 ± 0.4 ($P = 3.1$ E-09)	12.5 ± 1.1 (ns)	49.2 ± 3.1 ($P = 0.0255$)	nd	nd	nd	nd
D1o1-3 (L)	15.7 ± 1.9 (ns)	3.1 ± 0.4 ($P = 0.0011$)	10.9 ± 1.5 (ns)	nd	4.1 ± 0.3 ($P = 1.5$ E-09)	11.6 ± 2.4 (ns)	54.5 ± 6.7 (ns)	nd	nd	nd	nd
D1o3-1 (L)	14.8 ± 0.5 ($P = 0.0002$)	3.1 ± 0.1 ($P = 1.1$ E-05)	11 ± 0.9 (ns)	nd	4 ± 0.2 ($P = 1.9$ E-10)	19.7 ± 1.4 ($P = 1.04$ E-06)	47.4 ± 4.8 ($P = 0.0197$)	nd	nd	nd	nd
D1o3-3 (L)	14 ± 0.3 ($P = 6.2$ E-06)	2.1 ± 0.2 ($P = 1.3$ E-08)	8.8 ± 0.3 ($P = 6.4$ E-05)	nd	12.2 ± 0.5 ($P = 2.7$ E-13)	29 ± 0.3 ($P = 6.2$ E-12)	32.4 ± 0.9 ($P = 1.8$ E-07)	0.2 ± 0.04	0.3 ± 0.07	0.5 ± 0.02	0.4 ± 0.03
Wild type (R)	22.8 ± 0.5	0.3 ± 0.02	nd	1 ± 0.07	2.6 ± 0.2	39.2 ± 1.3	28.5 ± 1.6	nd	3.3 ± 0.3	2.5 ± 0.2	nd
D1o3-3 (R)	15.7 ± 0.3 ($P = 2.0$ E-11)	0.4 ± 0.1 (ns)	nd	2.8 ± 0.1 ($P = 9.1$ E-11)	12.8 ± 0.6 ($P = 6$ E-11)	45.9 ± 1 ($P = 1.5$ E-06)	17.8 ± 0.7 ($P = 3.2$ E-08)	nd	2.5 ± 0.1 ($P = 9.8$ E-05)	1.6 ± 0.1 ($P = 8.5$ E-07)	0.5 ± 0.1
Wild type (L-TAG)	37.0 ± 3.4	nd	nd	nd	8.8 ± 2.2	23.7 ± 5.1	30.5 ± 1.4	nd	nd	nd	nd
D1o3-3 (L-TAG)	12.5 ± 0.05 ($P = 7.5$ E-06)	0.9 ± 0.01	1.6 ± 0.03	1.6 ± 0.01	14.5 ± 0.01 ($P = 0.0022$)	35.6 ± 0.2 ($P = 0.0035$)	29.7 ± 0.09 ($P = 0.2936$)	0.7 ± 0.07	0.8 ± 0.02	0.8 ± 0.1	1.2 ± 0.08
Wild type (R-TAG)	nd	nd	nd	nd	nd	nd	nd	nd	nd	nd	nd
D1o3-3 (R-TAG)	15.1 ± 0.1	0.7 ± 0.02	nd	5.7 ± 0.2	21.6 ± 0.2	37.1 ± 0.4	14.1 ± 0.2	0.3 ± 0.03	3.1 ± 0.1	1.4 ± 0.1	0.8 ± 0.02

phase (48 h), this amounted to 8% to 9% and 22% to 23% more fatty acid per cell and more fatty acid produced per liter than AtD+o0-0 and AtD, respectively (Fig. 4, B and C).

The fatty acid profiles of the AtD, AtD+o0-0, and AtD +o3-3 cultures varied in a similar manner throughout their growth; the largest change occurred between 0 and 6 h of growth, which was seen by an increase (approximately 7%) in the proportion of 16:0 and a similar decrease in the proportion of 16:1 (Supplemental Table S1). By the early stationary phase, the proportion of 16:0 had returned to close to starting levels, whereas the proportion of 16:1 remained low after the initial decline.

Cys-Oleosins Are Targeted to Lipid Droplets and Are Cross Linked in Vivo

LDs from D1o3-3 leaf and root extracts were concentrated by flotational centrifugation. SDS-PAGE/immunoblot analysis revealed that in both organs, the Cys-oleosin was enriched in the LD fractions (Fig. 5A), indicating that the targeting process was not impaired by the addition of Cys residues. Similarly, the oleosins (o0-0 and o3-3) were both enriched in the LD fraction from *S. cerevisiae* (Fig. 4D). Prior to SDS-PAGE, it was essential to add reducing agent to any sample containing o3-3, indicating that the Cys-oleosins were cross linked in vivo via disulfide bonds in leaves, roots, and yeast.

The presence of Cys-oleosin in the insoluble cell debris fraction from both leaves and roots suggests that a considerable portion of the protein remained associated with the ER. This likely includes both immature LDs in the microsomal fraction as well as mature LDs that formed disulfide bonds with integral membrane proteins (Fig. 5A).

LDs from D1o3-3 Leaves and Roots Were Highly Resistant to Cys Protease But Only Partially Resistant to Ser Protease

During seed germination, the process of TAG mobilization is facilitated by LD-associated Cys proteases (EC 3.4.22), which in some cases preferentially degrade specific oleosins (Sadeghipour and Bhatla, 2002). We tested the integrity of isolated leaf and root LDs when incubated with a common plant Cys protease (papain) as well as the broad-spectrum Ser protease (EC 3.4.21), proteinase K (PNK). After 20 h of incubation in papain, the D1o3-3 LDs were essentially still fully intact, whereas approximately 35% of the TAG from the control LDs had escaped into the surrounding medium (Fig. 5B). After a similar incubation in PNK, approximately 25% and 50% of the TAG had escaped from the D1o3-3 and control LDs, respectively (Fig. 5B).

Immunoblot analysis revealed that when the D1o3-3 LDs were incubated in papain, the Cys-oleosin was rapidly but only partially degraded, leaving two discrete truncated forms, both of which appeared to be relatively resistant to further degradation (Fig. 5C). Like the full-length Cys-oleosin, these fragments could only be analyzed by SDS-PAGE after the addition of reducing agent to the sample. In contrast, incubating purified

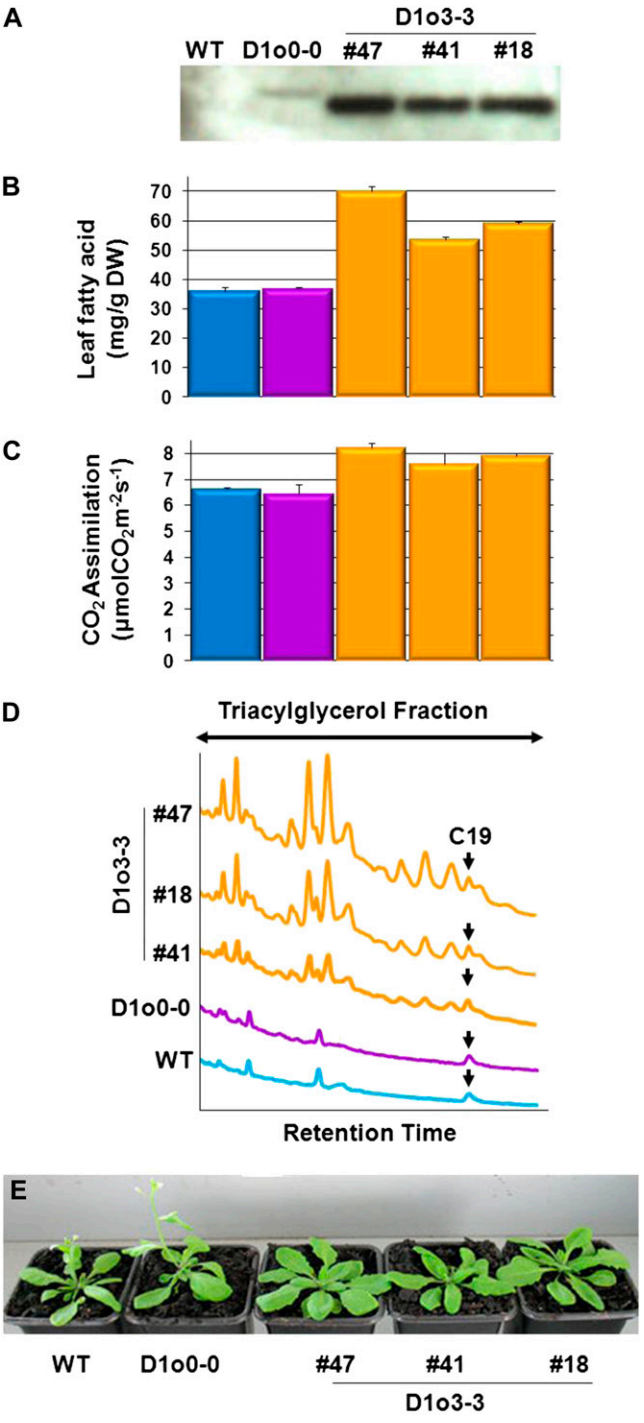

Figure 3. Relationship between the accumulation of recombinant Cys-oleosin o3-3 in leaves and leaf fatty acid content; TAG accumulation in the leaf; leaf CO_2 assimilation rate; and the overall influence on flower emergence and plant size. A to D show results from 35-DAS leaf tissue, while E shows plants at 25 DAS. Time point 35 DAS is the middle of flower production for all plants, and as such, we consider the leaves of these plants to be approximately the same physiological age. A, Immunoblot of total soluble leaf proteins extracted from the wild type (WT), D1o0-0, and three independent lines of D1o3-3 plants probed with polyclonal anti-o0-0 antibodies (Scott et al., 2010). B, Total fatty acid levels in leaves from the same group of plants in A. Bars represent mean values ± SD of separate experiments (n = 6), with statistical significance between the wild type and D1o3-3 lines calculated by Student's two-tailed t test. For D1o3-3 #18, #41, and #47, P = 1.12 E-11, 4.02 E-10, and 4.32 E-12, respectively. DW, Dry weight. C, Leaf CO_2 assimilation rates from the same group of plants in A. Bars represent mean values ± SD of separate experiments (n = 8), with statistical significance between the wild type and D1o3-3 lines calculated by Student's two-tailed t test. For D1o3-3 #18, #41, and #47, P = 9.15 E-09, 0.01698, and 8.7 E-08, respectively. D, Overlaid total ion chromatogram traces of TAGs extracted from equal quantities of dry leaf material from the same group of plants in A. Arrows indicates the C19 TAG internal standard. E, Photographs of representative plants at 25 DAS. Flower emergence is delayed by 2 to 3 d in D1o3-3 plants compared with the wild type and D1o0-0; however, the leaf biomass of the D1o3-3 plants is approximately 50% greater.

wild-type sesame seed LDs in papain resulted in the rapid and total disappearance of native sesame seed oleosin (Fig. 5C).

DISCUSSION

When we expressed DGAT1 in the leaf, we first assumed that this would in turn increase the demand of de novo leaf fatty acid biosynthesis and the subsequent formation of TAG (Winichayakul et al., 2008). However, in order to prevent TAG lipolysis and enable its long-term accumulation in leaves, we went on to suggest that it may be possible to exploit the seed LD structural protein, oleosin (Winichayakul et al., 2008; Dyer et al., 2012). In this study, we have compared the effects of constitutively expressing DGAT1 alone with constitutively coexpressing both DGAT1 and either unmodified oleosin or synthetically stabilized oleosins in plant vegetative organs and yeast. Oleosin was stabilized by placing between one and seven Cys residues in each of the amphipathic arms to create Cys-oleosins. The oleosins o0-0 and o1-1 appeared to have little effect, while D1o1-3 and D1o3-1 plants had relatively modest increases in leaf fatty acid, which declined as the leaves aged. D1o5-6 and D1o6-7 plants had higher levels as well, but they produced aberrant phenotypes that typically failed to produce seed. Only the coexpression of DGAT1 and o3-3 Cys-oleosins enabled the long-term elevation of fatty acid in the leaf, seen as 1.3-, 1.9-, and 3.4-fold increases in the total fatty acid content of expanding (14-DAS), mature (35-DAS), and senescent (91-DAS) leaves, respectively. In the mature leaves, this coincided with the accumulation of TAG to 2.1% (dry weight), or 44-fold higher than the wild type.

Fatty acid biosynthesis in green tissues was shown to use 3-phosphoglyceric acid synthesized by Rubisco (without the Calvin cycle; Schwender et al., 2004). This prompted Durrett et al. (2008) to speculate that increasing the de novo synthesis of free fatty acids in photosynthetic tissue could lead to an increase in CO_2 assimilation. This has not been realized until now, where we observed that the mature leaves of D1o3-3 fixed 24% more CO_2 m^{-2} s^{-1} and had a subsequent

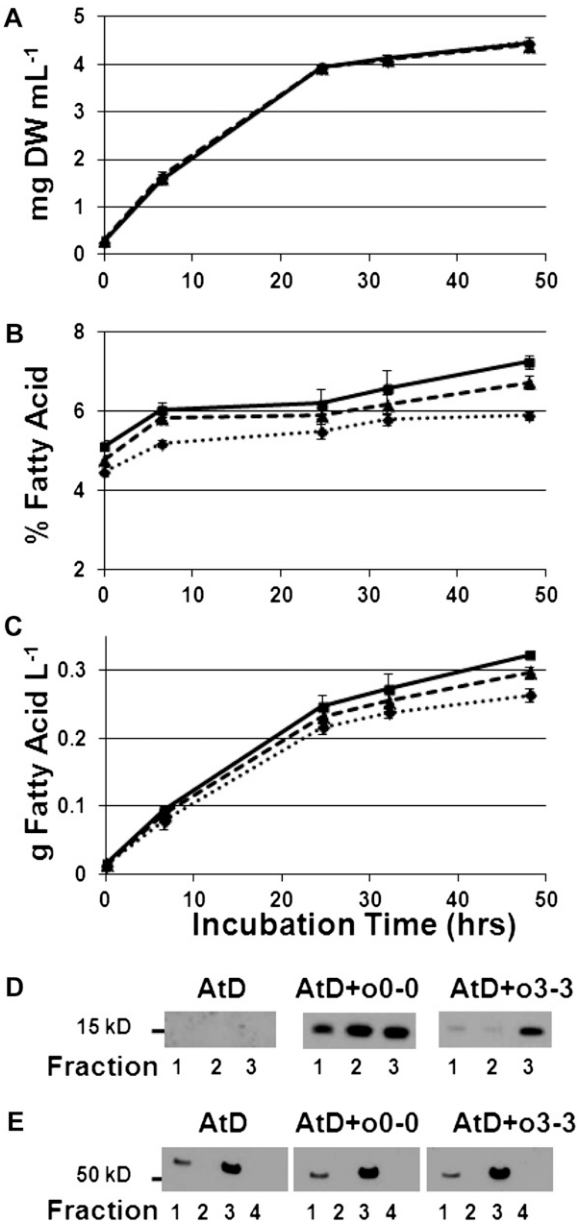

Figure 4. Growth and lipid data for yeast expressing AtD, AtD+o0-0, and AtD+o3-3, and localization of recombinant oleosins and DGAT1. A to C, Constitutive expression of AtD (diamonds, dotted line), AtD+o0-0 (triangles, dashed line), and AtD+o3-3 (squares, solid line). Curves represent mean values ± SD of separate experiments ($n = 3$), with statistical significance between cultures at the 48-h time point calculated by Student's two-tailed t test. A, Growth of cultures (mg dry weight [DW] mL^{-1}). B, Fatty acid content per cell (on a % dry weight basis). AtD+o0-0, $P = 2.5$ E-03; AtD+o3-3, $P = 2.9$ E-04. C, Fatty acid production per culture (g fatty acid L^{-1}). AtD+o0-0, $P = 0.0126$; AtD +o3-3, $P = 8.8$ E-04. D and E, Induced expression of AtD, AtD+o0-0, and AtD+o3-3. D, Anti-o0-0 antibody (Scott et al., 2010) probed immunoblots of crude cell extract + β-mercaptoethanol (fraction 1), LD preparation − β-mercaptoethanol (fraction 2), and LD preparation + β-mercaptoethanol (fraction 3). In order to detect o3-3 in the AtD+o3-3 crude cell extract, it was necessary to load four times the equivalent extraction volume compared with the LDs; consequently, the same procedure was performed for all crude cell extracts. No signal was detected in fractions from AtD cultures, while o3-3 showed a strong enrichment only in the LD + β-mercaptoethanol fraction, demonstrating its association with these organelles and its disulfide bond cross-linked status. On the other hand, o0-0 showed enrichment in both LD fractions (±β-mercaptoethanol), indicating that while it is associated with the LDs, it does not form disulfide bonds. The degree of enrichment of o0-0 in the LDs appears to be considerably less than that of o3-3; however, this more than likely reflects the combined effect of loading four times as much sample in the crude extract samples and the reduced sensitivity of the antibodies to o3-3 relative to o0-0 (S. Winichayakul and N.J. Roberts, unpublished data) rather than any differences in recombinant protein expression level. E, Anti-V5 antibody (Life Technologies) probed immunoblots of fraction 1 (crude extract), fraction 2 (LD preparation), fraction 3 (microsomal pellet extract), and fraction 4 (supernatant); equivalent extract volumes were loaded in each lane. Microsomal fractions show enrichment of DGAT1, demonstrating its association with the ER and not the LDs.

50% increase in total leaf biomass compared with the wild type. We suggest that in the absence of Cys-oleosin, the TAG produced by overexpressing DGAT1 is rapidly hydrolyzed by lipases and a portion of the resultant free fatty acid reenters the ER, where it is reincorporated into TAG. This establishes a futile cycle of TAG biosynthesis/hydrolysis that would negate the need to increase the level of de novo fatty acid biosynthesis and, therefore, prevent the predicted elevation of CO_2 assimilation. In comparison, the coexpression of DGAT1 and o3-3 results in the formation of stable LDs that prevent the hydrolysis of TAG and, as such, create a constant demand for elevated de novo fatty acid biosynthesis. In turn, this increases the CO_2 level in the chloroplast, enabling a higher CO_2 fixation rate and biomass production (Fig. 6).

The elevation in D1o3-3 leaf biomass (approximately 50%) is comparable to that achieved when either a portion of or the complete *Escherichia coli* glycolate catabolic pathway was engineered into Arabidopsis (approximately 30% and 60% increases, respectively; Kebeish et al., 2007) or when Arabidopsis was grown in a high-CO_2 environment (56% increase; Van der Kooij and De Kok, 1996). It is interesting that the three very different approaches (i.e. elevating the de novo biosynthesis of lipids in green tissues; reducing the flux of photorespiratory metabolites through peroxisomes and mitochondria; and elevating ambient CO_2) should achieve similar biomass gains over the wild type, which suggests that this may be close to the maximum achievable through increasing the efficiency of CO_2 capture. While we were unable to detect TAG in wild-type roots, it accumulated to 6.5% (dry weight) in D1o3-3 roots. This indicates that the coexpression of DGAT1 and Cys-oleosin can create a substantial sink in nonphotosynthetic tissue and that, in these plants, there was sufficient fatty acid- and TAG-synthesizing capacity in the roots as well as photosynthate available. The latter was presumably in part due to elevated CO_2 assimilation. We have yet to determine if the 2- to 3-d delay in flower emergence reflects the relative sink strengths of the various organs on the D1o3-3 plants. The subsequent

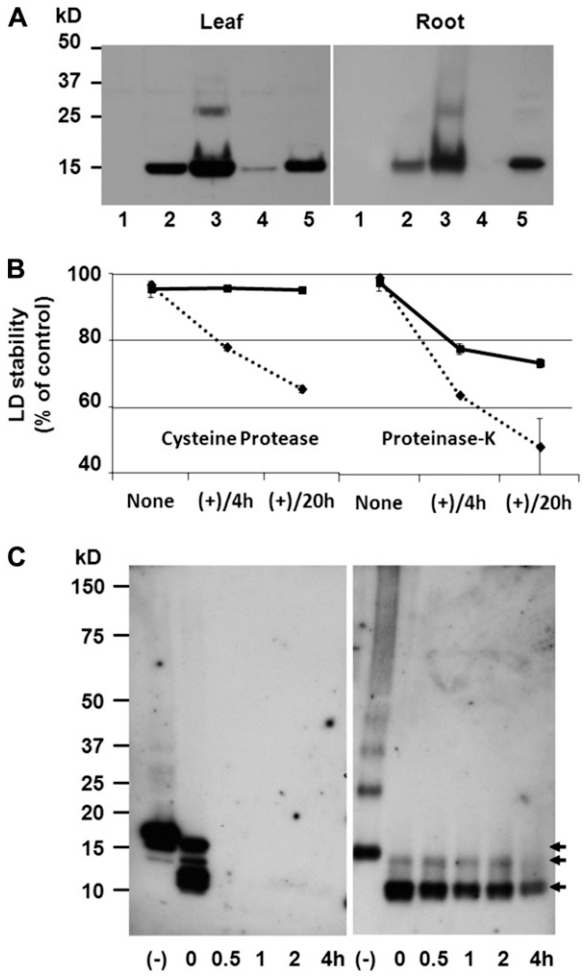

Figure 5. Colocalization of Cys-oleosins and LDs, and LD stability in proteases. A, Anti-o0-0 antibody (Scott et al., 2010) probed immunoblots of wild-type crude extract (lane 1), D1o3-3 crude extract (lane 2), D1o3-3 LD fraction (lane 3), D1o3-3 soluble fraction (lane 4), and D1o3-3 insoluble fraction (lane 5); equal quantities of protein were loaded per lane. LD fractions showed enrichment of o3-3, demonstrating its association with these artificial organelles. B, LD stability is shown as the percentage of TAG remaining in the LDs relative to preincubation. D1o3-3 LDs are shown by squares and solid line, and wild-type sesame seed LDs (control) are shown by diamonds and dotted line. Curves represent mean values ± SD of separate experiments (n = 2), with statistical significance between wild-type and D1o3-3 LDs calculated by Student's two-tailed t test: Cys protease 4 h and 20 h, P = 0.0021 and 0.0006, respectively; PNK 4 h and 20 h, P = 0.0071 and 0.0538, respectively. C, Immunoblots of leaf LDs incubated with Cys protease. Centrifuge-purified LDs (without denaturing or reducing agents) from wild-type sesame seeds (left panel) or D1o3-3 leaves (right panel) were incubated with Cys protease. Proteins were separated by SDS-PAGE under reducing conditions and probed with anti-o0-0 antibodies (Scott et al., 2010). The top arrow (15.2 kD) indicates undigested oleosins, and the middle and bottom arrows indicate relatively stable forms of papain-digested o3-3.

development of D1o3-3 flowers, however, suggests that sink strength is not limiting post emergence.

The resistance of o3-3 to Cys protease may explain why TAG was able to accumulate in leaves and, indeed, was still present in senescing leaves, where it has been previously estimated that as much as 37% of the senescence-associated ESTs are Cys proteases and 3% are lipases (Buchanan-Wollaston, 1997; Guo et al., 2004). Immunoblot analysis of papain-treated LDs combined with fatty acid and TAG accumulation data from leaves expressing different Cys-oleosins provide a possible mechanism to explain the Cys protease resistance of o3-3. When LDs from D1o3-3 vegetative tissue were incubated in Cys protease, the integrity of the LDs remained unaltered, although the full-length o3-3 was rapidly replaced by two smaller (10–11 and 13–14 kD) relatively stable forms of the protein. These forms match the predicted sizes of the hydrophobic core plus amphipathic arms shortened to the innermost Cys residues and the middle Cys residues, respectively. The longevity of the smallest fragment and the need to add reducing agent prior to SDS-PAGE suggest the innermost Cys residues form interoleosin disulfide bonds, creating regions on either side of the hydrophobic domain that are essentially protected from Cys protease degradation. When one of the inner Cys residues is absent, as in the case of o1-1, o1-3, and o3-1, the coexpression with DGAT1 results in relatively small and somewhat temporary increases in leaf fatty acids and TAG. The possibility of expressing truncated amphipathic arms or only engineering the pair of inner Cys residues has not yet been investigated; it should be remembered, however, that truncation may influence both targeting and topology and, therefore, LD formation. Furthermore, although we used the sesame L-oleosin, which is the isoform reported to not be ubiquitinated, as opposed to the H-oleosin isoform (Hsiao and Tzen, 2011), we cannot rule out the possibility that the Cys residues may also prevent ubiquitination of the Cys-oleosins.

In *S. cerevisiae*, the highest accumulation of fatty acids occurred in cells overexpressing AtD+o3-3 > AtD+o0-0 > AtD. Both Cys-oleosin and native oleosin were targeted to the yeast LDs, and, like the leaf and root LDs, the o3-3 in the LDs was oligomerized. It was previously suggested that the reason heterologous expression of caleosin (related to oleosin) in yeast cells resulted in higher lipid content was due to the interference with lipase (Froissard et al., 2009); this may also explain our data, where the cross linking of o3-3 would likely provide the greatest protection.

In eukaryotes, the formation of TAG via the Kennedy pathway involves the sequential acylation of glycerol-3-phosphate (Kennedy, 1961; Ohlrogge et al., 1991); the first steps are shared with the synthesis of polar glycerolipids, while the last step (performed by DGAT) is specific to the formation of TAG. The relatively low portions of 16:1 and 16:3 in the D1o3-3 leaf TAG demonstrates that the de novo fatty acyl residues reside mainly in the ER-based DAG and

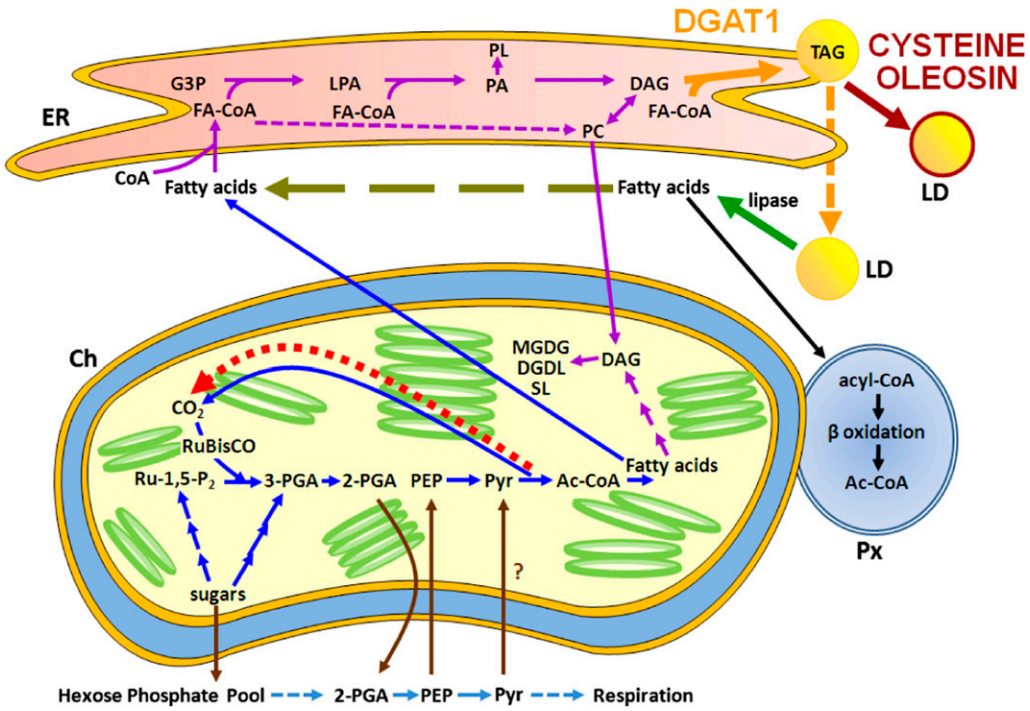

Figure 6. Schematic representation of interacting fatty acid metabolic pathways in wild-type, D1, and D1o3-3 leaves. It is anticipated that the generation and maintenance of thylakoid membranes in all leaves would require approximately the same degree of de novo fatty acid biosynthesis (blue pathway) and glycerolipid biosynthesis (purple pathway). The overexpression of DGAT (solid orange arrow) in D1 leads to the synthesis of TAG and the formation LDs (dashed orange arrow). However, in the absence of a suitably modified oleosin (D1 leaves), the LDs are unprotected from endogenous lipases, which results in the release of fatty acids (green arrow) into the cytoplasm, which are then normally degraded by β-oxidation in the peroxisome (black pathway). The overexpression of DGAT, however, creates an ongoing demand for elevated fatty acids in the ER. While these fatty acids would have originally been sourced from de novo biosynthesis, due to the lipase activity, they could now come from the TAG-released cytoplasmic pool (olive long dashed arrow). This creates a futile cycle of TAG biosynthesis/hydrolysis and reduces the quantity of additional de novo fatty acids required for TAG biosynthesis in D1 leaves. In contrast, the coexpression of DGAT and Cys-oleosin in D1o3-3 leaves leads to the formation of stable LDs (dark red arrow), which prevent the exposure of the TAG core to endogenous lipases. Combined with the continual expression of DGAT, this creates a sustained demand for fatty acids that elevates de novo biosynthesis (blue pathway). In turn, this results in an increase in the recycling of CO_2 from pyruvate within the chloroplast (bright red short dashed arrow). The consequence of this is an increase in the rate of CO_2 assimilation. It should be noted that since Arabidopsis plastids appear to lack enolase, which converts 2-phosphoglyceric acid to phospho*enol*pyruvate (PEP; Prabhakar et al., 2010), we have included a number of potential transporters (brown arrows), including the PEP/phosphate translocator (Flügge et al., 2011), to allow the model to utilize the cytosolic glycolysis pathway (light blue pathway) to convert 2-phosphoglyceric acid to PEP. This includes a potential pyruvate cytosol-plastid transportation step (shown by the question mark), as reviewed by Chapman et al. (2013). Ac-CoA, Acetyl-coenzyme A; Ch, chloroplast; DGDG, digalacto diglyceride; FA-CoA, fatty acid-coenzyme A; G3P, glycerol-3-phosphate; LPA, lysophosphatidic acid; MGDG, monogalacto diglyceride; PA, phosphatidic acid; PC, phosphatidylcholine; 2-PGA, 2-phosphoglyceric acid; 3-PGA, 3-phosphoglyceric acid; PL, phospholipid; Px, peroxisome; Pyr, pyruvate; Ru-1,5-P_2, ribulose-5-phosphate; SL, sphingolipid.

phosphatidylcholine and not in plastidial lipids. Given the early branch point of DAG to TAG synthesis, it could be expected that if TAG formation was occurring via the most direct route, then the majority of fatty acids in the TAG would be 18:1 and 16:0. However, the significantly elevated levels of 18:2 in both leaves and roots reveal that a considerable portion of TAG biosynthesis involves acyl cycling (less so in the roots) rather than direct de novo synthesis (Bates et al., 2007; Bates and Browse, 2011). Likewise, Arabidopsis seedlings that were modified to overexpress the seed maturation transcription factor *LEC1* also had reduced proportions of 16:0 and 18:3 and increased proportions of 18:1 and 18:2 (Mu et al., 2008). The degree of acyl cycling may not be the same in all leaf material, however. For example, the overexpression of either *DGAT1* or *LEC2* in tobacco resulted in dramatic increases in the proportion of 18:1 and corresponding decreases in the proportion of 18:3 in the leaf lipid but not in the transformed high-sugar cultivar NC-55 (Andrianov et al., 2010).

The overexpression of DGAT1 in tobacco leaves not only resulted in the accumulation of TAG but also greatly elevated the levels of two classes of

phospholipids, phosphatidylcholines and phosphatidylethanolamines, while reducing the level of the direct precursor of both TAG and phosphatidic acid phospholipids (Andrianov et al., 2010). Similarly, we observed that approximately 35% of the additional leaf lipid in D1o3-3 appeared to be in the form of polar glycerolipids and not as TAG, whereas the entire additional lipid in the roots appeared to be TAG. The accumulation of polar glycerolipids in the leaves may be a consequence of the relatively high maintenance of the leaf thylakoid membranes, which in Arabidopsis has been estimated to turn over at up to 4% per day (Bao et al., 2000). Thylakoid membrane fatty acids in Arabidopsis and tobacco can come from either the "prokaryotic" pathway within the chloroplast or from the "eukaryotic" pathway, where fatty acids are processed on ER-localized phosphatidylcholine and the DAG moiety is then returned to the chloroplast. By comparison, many agronomically important species predominantly use the eukaryotic pathway (Mongrand et al., 1998), and it is not yet known if the coexpression of DGAT1 and Cys-oleosin will result in a similar TAG-polar glycerolipid ratio in these plants.

The presence of VLCFAs in D1o3-3 leaves is interesting, as they are normally associated with Arabidopsis seeds and have been reported in leaves overexpressing *LEC2*, which was assumed to trigger their synthesis (Mu et al., 2008; Santos-Mendoza et al., 2008; Slocombe et al., 2009). At this stage, we have not determined if the expression of D1o3-3 triggers the synthesis of VLCFAs or if they are naturally present at very low levels (perhaps as wax ester precursors) and accumulate to detectable levels in the stabilized LDs. Furthermore, the decrease in overall proportion of VLCFAs but detection of two additional species in the D1o3-3 roots compared with the wild type does not completely rule out either possibility. In contrast to Arabidopsis, no new fatty acid species were detected in any of the yeast cultures expressing DGAT1. Instead, changes to the lipid profiles occurred predominantly during exponential growth and was seen as an increase in the proportion of 16:0. Thus, in yeast, the TAG biosynthesis proceeds with a minimum of acyl cycling and predominantly utilizes the first available newly synthesized lipid species (16:0).

CONCLUSION

By coexpressing a synthetically modified structural protein (Cys-oleosin) and DGAT1, we have substantially enhanced the energy densification of plant vegetative organs and yeast cells through the accumulation of TAG in stable artificial organelles. Furthermore, the coexpression led to an increase in leaf biomass that was comparable to that achieved by reducing the flux of photorespiratory metabolites through peroxisomes and mitochondria (Kebeish et al., 2007) or growing plants at elevated CO_2 (Van der Kooij and De Kok, 1996). Thus, Cys-oleosin has the potential to change the nutritional value of leafy materials and traditional starch food crops (e.g. potato [*Solanum tuberosum*], rice [*Oryza sativa*], maize [*Zea mays*]) as well as to increase biomass (particularly in C3 species). Moreover, there are a number of other plant modifications that may be complemented by the coexpression of Cys-oleosin. These include coexpression with both DGAT and mammalian monoacyglycerol acyltransferase, where heterologous in planta expression of the latter was shown to produce DAG from glycerol-3-phosphate that is independent of the Kennedy pathway (Petrie et al., 2012). Likewise, coexpression of Cys-oleosin and DGAT in switchgrass (*Panicum virgatum*) may benefit from the expression of the maize *Corngrass1* microRNA, which promotes juvenile cell wall identity and elevated starch (Chuck et al., 2011). Similarly, Cys-oleosin may complement modified microorganisms such as the *S. cerevisiae SUCROSE NON-FERMENTING2* (*SNF2*; a transcription factor involved in lipid accumulation) mutant coexpressing *Dga1* (a DGAT2; Kamisaka et al., 2007) or be coexpressed with *Dga2* (a DGAT1) in the oleaginous yeast species *Yarrowia lipolytica* (Beopoulos et al., 2011). Thus, the technology has broad applications in the biofuels, human, and animal feed industries.

MATERIALS AND METHODS

Binary Construct Design

Mammals, plants, and some yeasts possess two major forms of DGAT (DGAT1 and DGAT2; Beopoulos et al., 2011; Cao, 2011), which have unrelated primary sequences but catalyze the same reaction (the esterification of *sn*-1,2-diacylglycerol with a long-chain fatty acyl-CoA) and are located in distinct but separate regions of the ER (Shockey et al., 2006). Typically, however, DGAT1 is the major TAG-synthesizing enzyme in both the seed and senescing leaf (Kaup et al., 2002); hence, we chose to express DGAT1 in both Arabidopsis (*Arabidopsis thaliana*) and *Saccharomyces cerevisiae*.

The native Arabidopsis DGAT1 (accession no. NP_179535) peptide sequence was expressed in yeast, while a single mutation (S205A) was introduced for expression in Arabidopsis (Xu et al., 2008). The oleosin and DGAT1 coding sequences were optimized for expression in Arabidopsis (Scott et al., 2010) and placed in tandem into the plant binary vector pRSh1 (Scott et al., 2010), each under the control of cauliflower mosaic virus 35s promoters (Supplemental Fig. S5). Similarly, the oleosins and DGAT1 sequences were optimized for expression in yeast and were placed into modified pYES2.1 vectors (Life Technologies) containing either back-to-back inducible or constitutive promoters (Supplemental Fig. S6).

The different oleosins (seven in total) were cloned into separate binary constructs already containing DGAT1; this placed the oleosin and DGAT1 in tandem (each under the regulation of its own cauliflower mosaic virus 35S promoter; Supplemental Fig. S5). Multiple independent homozygous Arabidopsis transformants were generated with each construct; leaves from these plants were initially analyzed for total fatty acid content and recombinant oleosin.

Plant Transformation

Agrobacterium tumefaciens (GV3101) was used to stably transform Arabidopsis ecotype Columbia. Seed selection and preliminary determination of recombinant oleosin expression by immunoblot were performed as per Scott et al. (2010).

Seeds were stratified at 4°C in the dark for 3 d and then germinated on soil with 14 h of light (200 μmol m^{-2} s^{-1} photosynthetically active radiation) and 22°C. For root sampling, plants were grown in a mixture of vermiculite and perlite (1:1) and fed with N-Hoagland solution. Southern-blot and segregation analyses were consistent with a single locus of insertion of the transfer DNA for each independent D1o3-3 line used in this comparison.

Yeast Transformation

S. cerevisiae strain INV-Sc 1 (Life Technologies) was transformed as per Elble (1992) and selected by the ability to grow in the absence of uracil. *S. cerevisiae* strain transformants were picked from a fresh plate lacking uracil and then grown in synthetic dropout medium lacking uracil for 30 to 40 h at 30°C, 200 rpm, and then diluted to an optical density at 600 nm of 0.4 in 500-mL cultures. At various time points, aliquots of the cultures were removed, centrifuged at 1,000*g*, frozen in liquid nitrogen, and stored at −80°C.

Lipid Extraction and Analysis

Approximately 10 mg of freeze-dried finely ground plant material was accurately weighed and then extracted in hot methanolic HCl for fatty acid methyl ester analysis (Browse et al., 1986). The process was similar for yeast, except that glass beads were used to disrupt the cells by vortexing for 1 min. For TAG analysis, 100 mg of dry material was extracted in a mixture of methanolic saline and heptane (Ruiz-López et al., 2003). The extract enables the comparative quantification of neutral lipids and some more polar glycerol lipids after separation on an MXT-65TG gas chromatography column (Restek 77008). Further partitioning of the TAGs from other lipids was achieved by hydrophobic column chromatography, which employed 1-mL solid-phase extraction columns containing 100 mg of silicon packing (Strata 8B-s012-EAK; Tonon et al., 2002). TAGs were eluted using a chloroform-hexane mixture and subjected to quantitative fatty acid methyl ester analysis.

Gross Energy Determination

The gross energy of the leaves was determined on freeze-dried, powdered samples pooled from multiple ($n > 30$) plants of the same line, germinated at the same time, and grown under the same conditions. Bomb calorimetry was performed by the International Accreditation New Zealand-approved Nutrition Laboratory at Massey University. Internal standards were included in each batch, and the uncertainty of measurement was determined as ±0.6%.

Gas-Exchange Analysis

Rates of CO_2 assimilation were measured from plants at 35 DAS using an infrared gas analyzer (Li6400; Li-Cor) fitted with a standard 2- × 3-cm leaf chamber, a leaf thermocouple, and a blue-red light-emitting diode light source at 200 μmol m^{-2} s^{-1} photosynthetically active radiation. Block temperature was held at 20°C, stomata ratio was set at 1.6, and the vapor pressure deficit was between 0.6 and 0.9 kPa.

LD Imaging

LDs in mesophyll tissue were visualized using confocal fluorescence microscopy. Plant material was vacuum infiltrated (70 kPa) for 5 min in 3.5% (w/v) paraformaldehyde in 1× phosphate-buffered saline (PBS), pH 7.4, then left in this fixative overnight at 4°C. Fixed samples were washed twice for 30 min each with 1× PBS and then once with 1% (v/v) Triton X-100 containing 1× PBS, stained for 30 min with 2.5 mg L^{-1} Nile Red in 75% glycerol, followed by a further wash in 1× PBS. For Nile Red imaging, excitation was at 495 nm and emission was at 530 and 600 nm.

LD Extraction

Approximately 1 g of fresh leaves or roots was ground with a mortar and pestle containing a spatula tip of washed sand and 2 mL of 2× grinding buffer (100 mM sodium phosphate buffer, pH 7.2, 300 mM NaCl, and 1.2 M Suc; 10 mg of cetyl-trimethyl-ammonium bromide was added for leaf samples). Samples were centrifuged (10,000*g*, 10 min, 22°C); the immiscible fat pad and underlying aqueous supernatant were transferred to a fresh tube and separated by repeat centrifugation. The aqueous layer was removed by pipetting, while the overlying LD fraction was washed (1× grinding buffer) and centrifuged several times, discarding the resultant aqueous layer and pellet between washes.

Yeast cells were diluted to an optical density at 600 nm of approximately 100 in extraction buffer (100 mM Tris, pH 7.5, 1 mM EDTA, 5% glycerol, 1 mM phenylmethylsulfonyl fluoride, and 1× protease Complete [Roche]) and vortexed with an equal volume of glass beads. Cell debris was pelleted at 1,000*g* for 5 min, and supernatant was added to an equal volume of 1.2 M sorbitol in ultracentrifuge tubes, mixed by inversion, and then centrifuged (100,000*g*, 60 min, 4°C).

SDS-PAGE Analysis of Oleosin, Cys-Oleosins, and LD Proteins

Protein samples were prepared by mixing fresh or lyophilized ground material with an equal volume of 2× loading buffer (1:2 diluted 4× lithium dodecyl sulfate sample buffer [Life Technologies], 8 M urea, and 5% [v/v] β-mercaptoethanol) and then an appropriate volume of water to achieve 1× loading buffer. Equal quantities of protein were separated by SDS-PAGE (NuPAGE Novex 4%–12% Bis-Tris precast gradient gels; Life Technologies) and stained by SimplyBlue Safe-Stain (Life Technologies) or blotted onto nitrocellulose using an iBlot (Life Technologies). The membrane was blocked in medium containing 5% (w/v) skim milk powder in Tris-buffered saline + Tween 20 (TBST; 50 mM Tris, pH 7.4, 100 mM NaCl, and 0.1% Tween 20) for at least 1.5 h (22°C), then washed in TBST for 10 min before incubating with a 1:200 dilution of rabbit anti-oleosin (Scott et al., 2010) or a 1:5,000 dilution of mouse anti-V5-horseradish peroxidase (Life Technologies) in M-TBST (1 h, 22°C), followed by three further washes (10 min each) in TBST. The membranes probed with rabbit anti-oleosin were then incubated with a 1:5,000 dilution of anti-rabbit IgG horseradish peroxidase-linked whole antibody from donkey (GE Healthcare NA934) in M-TBST (1 h, 22°C) before three final washes in TBST. Enzyme activity was visualized using chemiluminescence, exposed, and developed on Biomax Scientific Imaging Film (Kodak).

LD Stability Determination

LD stability was determined by quantifying the TAG released after exposure to either Cys protease (papain) or PNK as per Scott et al. (2010) with one modification, in which the volume of fish oil was reduced to 10 μL. LD integrity was determined after 37°C incubation with either PNK + buffer (10 mM Tris, pH 8, and 2 mM $CaCl_2$) or Cys protease + buffer (50 mM phosphate buffer, pH 7.2, 150 mM NaCl, and 2 mM EDTA). PNK:LD and Cys protease:LD protein ratios were 1:10, quantified by Qbit (Life Technologies).

Statistical Analysis

Statistically significant differences between transgenic lines and the wild type were calculated by Student's two-tailed *t* test. Error bars and ranges given are SD.

Sequence data from this article can be found in the GenBank/EMBL data libraries under accession numbers NP_179535 and AAD42942.

Supplemental Data

The following materials are available in the online version of this article.

Supplemental Figure S1. Comparison over time of TAG in leaves.

Supplemental Figure S2. Leaf phenotype of D1o5-6 and D1o6-7 seedlings.

Supplemental Figure S3. Comparison of TAG accumulation in roots versus leaves from plants cotransformed with DGAT1 and the Cys-oleosin o3-3.

Supplemental Figure S4. Comparison of polar glycerolipids accumulating in leaves of wild-type plants or plants transformed with DGAT1 and the Cys-oleosin o3-3.

Supplemental Figure S5. Construct design for coexpression of DGAT1 and oleosins in Arabidopsis.

Supplemental Figure S6. Construct designs for coexpression of DGAT1 and oleosins in *S. cerevisiae*.

Supplemental Table S1. Lipid profiles of *S. cerevisiae*, cultures sampled at 0-, 6.5-, 24-, 32-, and 48-h time points.

ACKNOWLEDGMENTS

We gratefully acknowledge helpful advice on the manuscript from Dr. Gregory Bryan (AgResearch), Prof. Katie Dehesh (University of California, Davis), Prof. Animesh Ray (Kek Graduate Institute), and Dr. David Taylor (National Research Council Canada).

Received February 26, 2013; accepted April 22, 2013; published April 24, 2013.

LITERATURE CITED

Andrianov V, Borisjuk N, Pogrebnyak N, Brinker A, Dixon J, Spitsin S, Flynn J, Matyszczuk P, Andryszak K, Laurelli M, et al (2010) Tobacco as a production platform for biofuel: overexpression of *Arabidopsis DGAT* and *LEC2* genes increases accumulation and shifts the composition of lipids in green biomass. Plant Biotechnol J **8:** 277–287

Athenstaedt K, Daum G (2006) The life cycle of neutral lipids: synthesis, storage and degradation. Cell Mol Life Sci **63:** 1355–1369

Bao X, Focke M, Pollard M, Ohlrogge J (2000) Understanding *in vivo* carbon precursor supply for fatty acid synthesis in leaf tissue. Plant J **22:** 39–50

Bates PD, Browse J (2011) The pathway of triacylglycerol synthesis through phosphatidylcholine in Arabidopsis produces a bottleneck for the accumulation of unusual fatty acids in transgenic seeds. Plant J **68:** 387–399

Bates PD, Ohlrogge JB, Pollard M (2007) Incorporation of newly synthesized fatty acids into cytosolic glycerolipids in pea leaves occurs via acyl editing. J Biol Chem **282:** 31206–31216

Beopoulos A, Nicaud J-M, Gaillardin C (2011) An overview of lipid metabolism in yeasts and its impact on biotechnological processes. Appl Microbiol Biotechnol **90:** 1193–1206

Bouvier-Navé P, Benveniste P, Oelkers P, Sturley SL, Schaller H (2000) Expression in yeast and tobacco of plant cDNAs encoding acyl CoA: diacylglycerol acyltransferase. Eur J Biochem **267:** 85–96

Brasaemle DL (2007) Thematic review series: adipocyte biology. The perilipin family of structural lipid droplet proteins: stabilization of lipid droplets and control of lipolysis. J Lipid Res **48:** 2547–2559

Browse J, McCourt PJ, Somerville CR (1986) Fatty acid composition of leaf lipids determined after combined digestion and fatty acid methyl ester formation from fresh tissue. Anal Biochem **152:** 141–145

Buchanan-Wollaston V (1997) The molecular biology of leaf senescence. J Exp Bot **48:** 181–199

Cao H (2011) Structure-function analysis of diacylglycerol acyltransferase sequences from 70 organisms. BMC Res Notes **21:** 249

Chapman KD, Dyer JM, Mullen RT (2013) Commentary: why don't plant leaves get fat? Plant Sci **207:** 128–134

Chisti Y (2007) Biodiesel from microalgae. Biotechnol Adv **25:** 294–306

Chuck GS, Tobias C, Sun L, Kraemer F, Li C, Dibble D, Arora R, Bragg JN, Vogel JP, Singh S, et al (2011) Overexpression of the maize Corngrass1 microRNA prevents flowering, improves digestibility, and increases starch content of switchgrass. Proc Natl Acad Sci USA **108:** 17550–17555

Czabany T, Athenstaedt K, Daum G (2007) Synthesis, storage and degradation of neutral lipids in yeast. Biochim Biophys Acta **1771:** 299–309

Durrett TP, Benning C, Ohlrogge J (2008) Plant triacylglycerols as feedstocks for the production of biofuels. Plant J **54:** 593–607

Dyer J, Mullen R, Chapman K (2012) Oil in biomass: a step-change for bioenergy. American Oil Chemists' Society. http://www.aocs.org/Membership/informArticleDetail.cfm?ItemNumber=18107 (May 9, 2013)

Eastmond PJ (2006) *SUGAR-DEPENDENT1* encodes a patatin domain triacylglycerol lipase that initiates storage oil breakdown in germinating *Arabidopsis* seeds. Plant Cell **18:** 665–675

Elble R (1992) A simple and efficient procedure for transformation of yeasts. Biotechniques **13:** 18–20

Flügge U-I, Häusler RE, Ludewig F, Gierth M (2011) The role of transporters in supplying energy to plant plastids. J Exp Bot **62:** 2381–2392

Fortman JL, Chhabra S, Mukhopadhyay A, Chou H, Lee TS, Steen E, Keasling JD (2008) Biofuel alternatives to ethanol: pumping the microbial well. Trends Biotechnol **26:** 375–381

Froissard M, D'Andréa S, Boulard C, Chardot T (2009) Heterologous expression of AtClo1, a plant oil body protein, induces lipid accumulation in yeast. FEMS Yeast Res **9:** 428–438

Gepstein S (2004) Leaf senescence: not just a 'wear and tear' phenomenon. Genome Biol **5:** 212

Goodman JM (2008) The gregarious lipid droplet. J Biol Chem **283:** 28005–28009

Granda CB, Zhu L, Holtzapple MT (2007) Sustainable liquid biofuels and their environmental impact. Environ Prog **26:** 233–250

Guo Y, Cai Z, Gan S (2004) Transcriptome of Arabidopsis leaf senescence. Plant Cell Environ **27:** 521–549

Hill J, Nelson E, Tilman D, Polasky S, Tiffany D (2006) Environmental, economic, and energetic costs and benefits of biodiesel and ethanol biofuels. Proc Natl Acad Sci USA **103:** 11206–11210

Hsiao ESL, Tzen JTC (2011) Ubiquitination of oleosin-H and caleosin in sesame oil bodies after seed germination. Plant Physiol Biochem **49:** 77–81

James CN, Horn PJ, Case CR, Gidda SK, Zhang D, Mullen RT, Dyer JM, Anderson RGW, Chapman KD (2010) Disruption of the Arabidopsis CGI-58 homologue produces Chanarin-Dorfman-like lipid droplet accumulation in plants. Proc Natl Acad Sci USA **107:** 17833–17838

Kamisaka Y, Tomita N, Kimura K, Kainou K, Uemura H (2007) DGA1 (diacylglycerol acyltransferase gene) overexpression and leucine biosynthesis significantly increase lipid accumulation in the Deltasnf2 disruptant of Saccharomyces cerevisiae. Biochem J **408:** 61–68

Kaup MT, Froese CD, Thompson JE (2002) A role for diacylglycerol acyltransferase during leaf senescence. Plant Physiol **129:** 1616–1626

Kebeish R, Niessen M, Thiruveedhi K, Bari R, Hirsch H-J, Rosenkranz R, Stäbler N, Schönfeld B, Kreuzaler F, Peterhänsel C (2007) Chloroplastic photorespiratory bypass increases photosynthesis and biomass production in *Arabidopsis thaliana*. Nat Biotechnol **25:** 593–599

Kennedy EP (1961) Biosynthesis of complex lipids. Fed Proc **20:** 934–940

Lin W, Oliver DJ (2008) Role of triacylglycerols in leaves. Plant Sci **175:** 233–237

Martin S, Parton RG (2006) Lipid droplets: a unified view of a dynamic organelle. Nat Rev Mol Cell Biol **7:** 373–378

Mongrand S, Bessoule J-J, Cabantous F, Cassagne C (1998) The $C_{16:3}/C_{18:3}$ fatty acid balance in photosynthetic tissues from 468 plant species. Phytochemistry **49:** 1049–1064

Mu J, Tan H, Zheng Q, Fu F, Liang Y, Zhang J, Yang X, Wang T, Chong K, Wang X-J, et al (2008) LEAFY COTYLEDON1 is a key regulator of fatty acid biosynthesis in Arabidopsis. Plant Physiol **148:** 1042–1054

Murphy DJ (2012) The dynamic roles of intracellular lipid droplets: from archaea to mammals. Protoplasma **249:** 541–585

Ohlrogge J, Allen D, Berguson B, Dellapenna D, Shachar-Hill Y, Stymne S (2009) Energy: driving on biomass. Science **324:** 1019–1020

Ohlrogge JB, Browse J, Somerville CR (1991) The genetics of plant lipids. Biochim Biophys Acta **1082:** 1–26

Peng CC, Lin IP, Lin CK, Tzen JTC (2003) Size and stability of reconstituted sesame oil bodies. Biotechnol Prog **19:** 1623–1626

Petrie JR, Vanhercke T, Shrestha P, El Tahchy A, White A, Zhou X-R, Liu Q, Mansour MP, Nichols PD, Singh SP (2012) Recruiting a new substrate for triacylglycerol synthesis in plants: the monoacylglycerol acyltransferase pathway. PLoS ONE **7:** e35214

Prabhakar V, Löttgert T, Geimer S, Dörmann P, Krüger S, Vijayakumar V, Schreiber L, Göbel C, Feussner K, Feussner I, et al (2010) Phosphoenolpyruvate provision to plastids is essential for gametophyte and sporophyte development in *Arabidopsis thaliana*. Plant Cell **22:** 2594–2617

Ruiz-López N, Martínez-Force E, Garcés R (2003) Sequential one-step extraction and analysis of triacylglycerols and fatty acids in plant tissues. Anal Biochem **317:** 247–254

Sadeghipour HR, Bhatla SC (2002) Differential sensitivity of oleosins to proteolysis during oil body mobilization in sunflower seedlings. Plant Cell Physiol **43:** 1117–1126

Sanjaya , Durrett TP, Weise SE, Benning C (2011) Increasing the energy density of vegetative tissues by diverting carbon from starch to oil biosynthesis in transgenic Arabidopsis. Plant Biotech J **9:** 874–883

Santos-Mendoza M, Dubreucq B, Baud S, Parcy F, Caboche M, Lepiniec L (2008) Deciphering gene regulatory networks that control seed development and maturation in Arabidopsis. Plant J **54:** 608–620

Schwender J, Goffman F, Ohlrogge JB, Shachar-Hill Y (2004) Rubisco without the Calvin cycle improves the carbon efficiency of developing green seeds. Nature **432:** 779–782

Scott RW, Winichayakul S, Roldan M, Cookson R, Willingham M, Castle M, Pueschel R, Peng CC, Tzen JTC, Roberts NJ (2010) Elevation of oil body integrity and emulsion stability by polyoleosins, multiple oleosin units joined in tandem head-to-tail fusions. Plant Biotechnol J **8:** 912–927

Shimada TL, Shimada T, Takahashi H, Fukao Y, Hara-Nishimura I (2008) A novel role for oleosins in freezing tolerance of oilseeds in *Arabidopsis thaliana*. Plant J **55:** 798–809

Shockey JM, Gidda SK, Chapital DC, Kuan J-C, Dhanoa PK, Bland JM, Rothstein SJ, Mullen RT, Dyer JM (2006) Tung tree DGAT1 and DGAT2 have nonredundant functions in triacylglycerol biosynthesis and are localized to different subdomains of the endoplasmic reticulum. Plant Cell **18:** 2294–2313

Siloto RMP, Findlay K, Lopez-Villalobos A, Yeung EC, Nykiforuk CL, Moloney MM (2006) The accumulation of oleosins determines the size of seed oilbodies in *Arabidopsis*. Plant Cell **18:** 1961–1974

Slocombe SP, Cornah J, Pinfield-Wells H, Soady K, Zhang Q, Gilday A, Dyer JM, Graham IA (2009) Oil accumulation in leaves directed by modification of fatty acid breakdown and lipid synthesis pathways. Plant Biotechnol J **7:** 694–703

Somerville C (2007) Biofuels. Curr Biol **17:** R115–R119

Tai SSK, Chen MCM, Peng CC, Tzen JTC (2002) Gene family of oleosin isoforms and their structural stabilization in sesame seed oil bodies. Biosci Biotechnol Biochem **66:** 2146–2153

Tonon T, Harvey D, Larson TR, Graham IA (2002) Long chain polyunsaturated fatty acid production and partitioning to triacylglycerols in four microalgae. Phytochemistry **61:** 15–24

Troncoso-Ponce MA, Cao X, Yang Z, Ohlrogge JB (2013) Lipid turnover during senescence. Plant Sci **205-206:** 13–19

Tzen JTC, Lie GC, Huang AHC (1992) Characterization of the charged components and their topology on the surface of plant seed oil bodies. J Biol Chem **267:** 15626–15634

Van der Kooij TAW, De Kok LJ (1996) Impact of elevated CO_2 on drowth and development of *Arabidopsis thaliana* L. Phyton **36:** 173–184

Welte MA (2007) Proteins under new management: lipid droplets deliver. Trends Cell Biol **17:** 363–369

Winichayakul S, Cookson R, Scott R, Zhou X, Zou X, Roldan M, Richardson K, Roberts N (2008) Delivery of grasses with high levels of unsaturated, protected fatty acids. Proc N Z Grassland Assoc **70:** 211–216

Xu JY, Francis T, Mietkiewska E, Giblin EM, Barton DL, Zhang Y, Zhang M, Taylor DC (2008) Cloning and characterization of an acyl-CoA-dependent diacylglycerol acyltransferase 1 (DGAT1) gene from *Tropaeolum majus*, and a study of the functional motifs of the DGAT protein using site-directed mutagenesis to modify enzyme activity and oil content. Plant Biotechnol J **6:** 799–818

Yang Z, Ohlrogge JB (2009) Turnover of fatty acids during natural senescence of Arabidopsis, Brachypodium, and switchgrass and in Arabidopsis β-oxidation mutants. Plant Physiol **150:** 1981–1989